

Supporting Information for

Guanidine-Functionalized Rhenium Cyclopentadienyl Carbonyl Complexes: Synthesis and Cooperative Activation of H–H and O–H Bonds

Thomas S. Teets, Jay A. Labinger* and John E. Bercaw*

Arnold and Mabel Beckman Laboratories of Chemical Synthesis, California Institute of Technology, Pasadena, CA 91125

<i>Index</i>	<i>Page</i>
X-ray crystallographic summary tables	S2–S3
HMBC spectrum for complex 8	S4
Plots for K_{eq} determination and partial VT NMR spectra for van't Hoff analysis	S5–S9
NMR spectra for all reported compounds	S10–S19

Table S1. Crystallographic summary for **1–3**.

	1	2	3
Formula	C ₁₃ H ₁₄ N ₃ O ₃ Re	C ₁₃ H ₁₅ BF ₄ N ₃ O ₃ Re	C ₁₂ H ₁₅ B ₂ F ₈ N ₄ O ₃ Re
fw, g/mol	446.47	534.29	623.10
Temperature/K	100(2)	100(2)	100(2)
cryst. syst.	Monoclinic	Monoclinic	Orthorhombic
space group	P2 ₁ /c	P2 ₁ /n	Pca2 ₁
color	Colorless	Colorless	Yellow
<i>a</i> /Å	9.8852(5)	8.1382(10)	21.1586(9)
<i>b</i> /Å	14.8057(7)	21.483(3)	7.8417(3)
<i>c</i> /Å	9.5666(5)	9.4361(12)	22.8621(10)
$\alpha/^\circ$	90	90	90
$\beta/^\circ$	104.348(2)	90.539(6)	90
$\gamma/^\circ$	90	90	90
<i>V</i> /Å ³	1356.47(12)	1649.7(4)	3793.3(3)
ρ (calc.)/(g cm ⁻³)	2.186	2.151	2.182
<i>Z</i>	4	4	8
no. refl.	42327	197454	118663
no. unique refl.	7027	13825	12650
<i>R</i> _{int}	0.0379	0.0451	0.0654
<i>R</i> ₁ ^a (all data)	0.0278	0.0233	0.0445
<i>wR</i> ₂ ^b (all data)	0.0462	0.0434	0.0888
<i>R</i> ₁ [(I > 2σ)]	0.0201	0.0189	0.0386
<i>wR</i> ₂ [(I > 2σ)]	0.0437	0.0422	0.0858
<i>GOF</i> ^c	1.019	1.122	1.120

^a $R_1 = \frac{\sum ||F_o - |F_c||/\sum |F_o|}{\sum |F_o|}$. ^b $wR_2 = \left(\frac{\sum (w(F_o^2 - F_c^2)^2)}{\sum w(F_o^2)^2} \right)^{1/2}$. ^c $GOF = \left(\frac{\sum w(F_o^2 - F_c^2)^2}{(n-p)} \right)^{1/2}$ where *n* is the number of data and *p* is the number of parameters refined.

Table S2. Crystallographic summary for **4** and **7**.

	4	7
Formula	C ₁₂ H ₁₄ BF ₄ N ₄ O ₃ Re	C ₁₃ H ₁₇ N ₄ O ₄ Re
fw, g/mol	535.28	479.51
Temperature/K	100(2)	100(2)
cryst. syst.	Monoclinic	Monoclinic
space group	<i>P</i> 2 ₁ /c	<i>P</i> 2 ₁ /c
color	Orange	Yellow
<i>a</i> /Å	11.1053(4)	8.3732(4)
<i>b</i> /Å	9.9635(3)	7.8158(4)
<i>c</i> /Å	14.9378(5)	23.0017(11)
α°	90	90
β°	95.2430(10)	95.791(2)
γ°	90	90
<i>V</i> /Å ³	1645.92(9)	1497.62(13)
ρ (calc.)/(g cm ⁻³)	2.160	2.127
<i>Z</i>	4	4
no. refl.	37996	137916
no. unique refl.	6279	11127
<i>R</i> _{int}	0.0365	0.0642
<i>R</i> ₁ ^a (all data)	0.0414	0.0470
<i>wR</i> ₂ ^b (all data)	0.0737	0.0700
<i>R</i> ₁ [(I > 2σ)]	0.0341	0.0345
<i>wR</i> ₂ [(I > 2σ)]	0.0699	0.0661
<i>GOF</i> ^c	1.148	1.085

^a $R_1 = \sum ||F_o - |F_c|| / \sum |F_o|$. ^b $wR_2 = (\sum (w(F_o^2 - F_c^2)^2) / \sum (w(F_o^2)^2))^{1/2}$. ^c $GOF = (\sum w(F_o^2 - F_c^2)^2 / (n - p))^{1/2}$ where *n* is the number of data and *p* is the number of parameters refined.

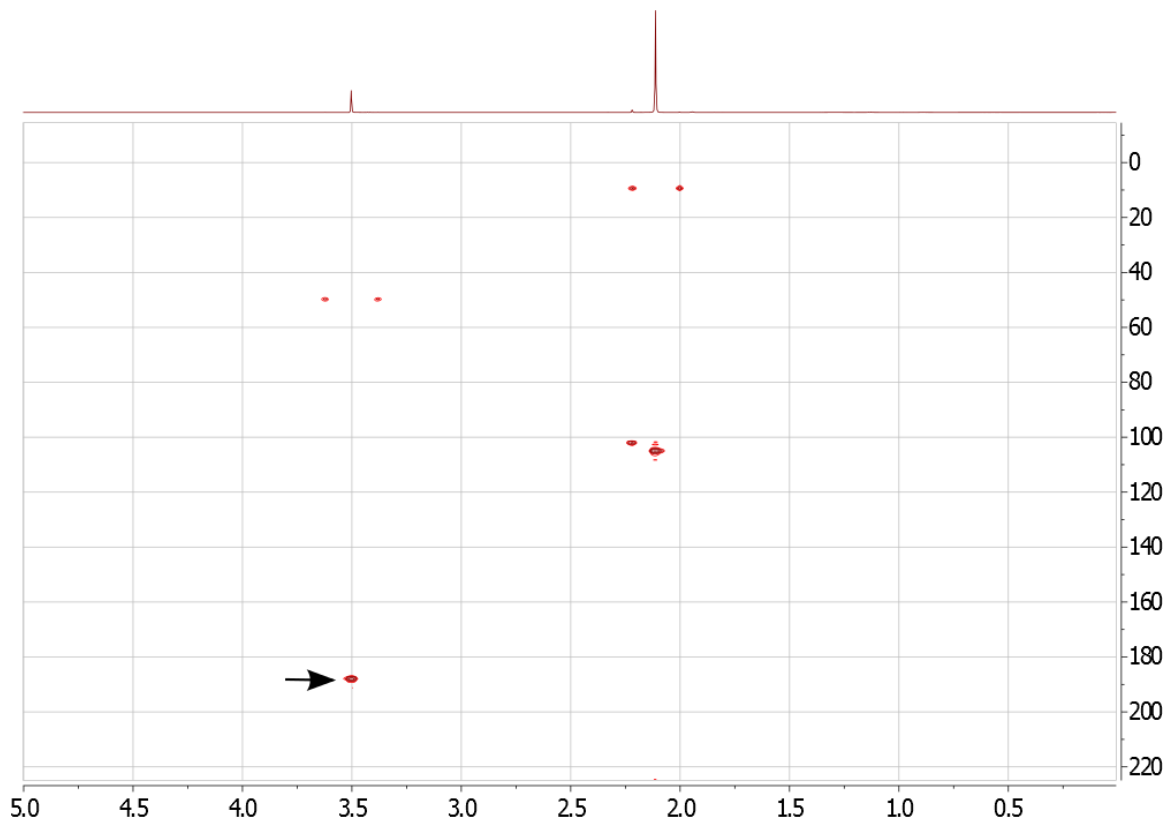


Figure S1. HMBC spectrum for methoxycarbonyl complex **8**, with ¹H chemical shift on the horizontal axis and ¹³C chemical shift on the vertical axis. The correlation between the methoxycarbonyl ¹H and ¹³C resonances is highlighted with an arrow.

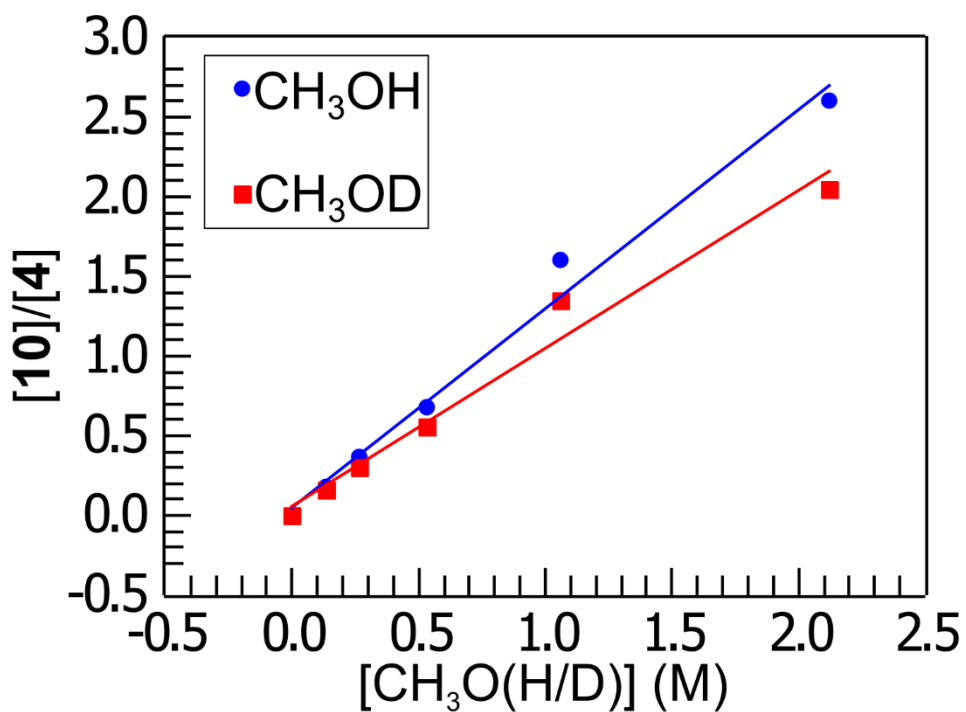


Figure S2. Plot of the ratio $[10]/[4]$ present at equilibrium when complex **4** (6.0 mM) is treated with varying concentrations of CH_3OH (●, blue) or CH_3OD (■, red). The best-fit lines, which were used to determine K_{eq} , are shown as solid lines of the same color.

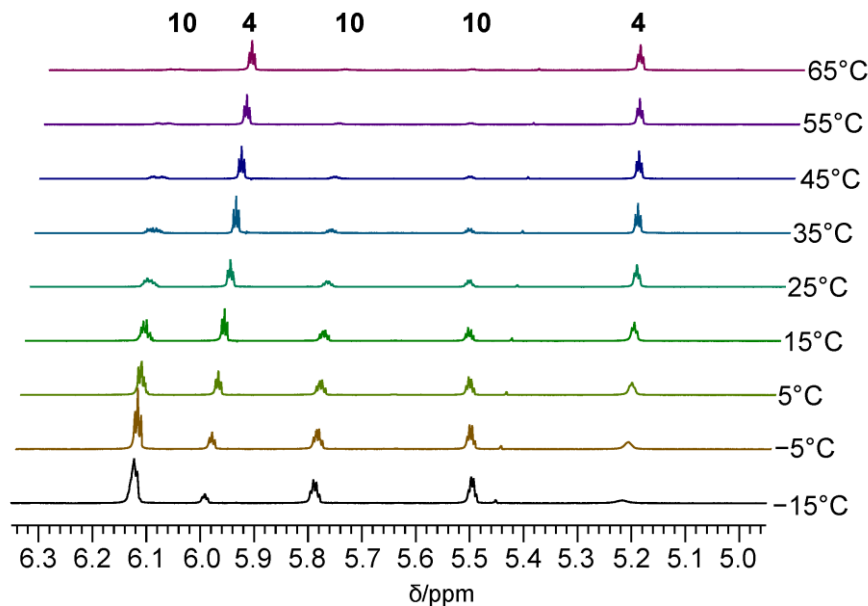


Figure S3. Partial variable-temperature ^1H NMR spectra for complex **4** in the presence of 0.60 M CH_3OH in CD_3CN . The cyclopentadienyl region is shown, with peaks attributed to **4** and **10** labeled.

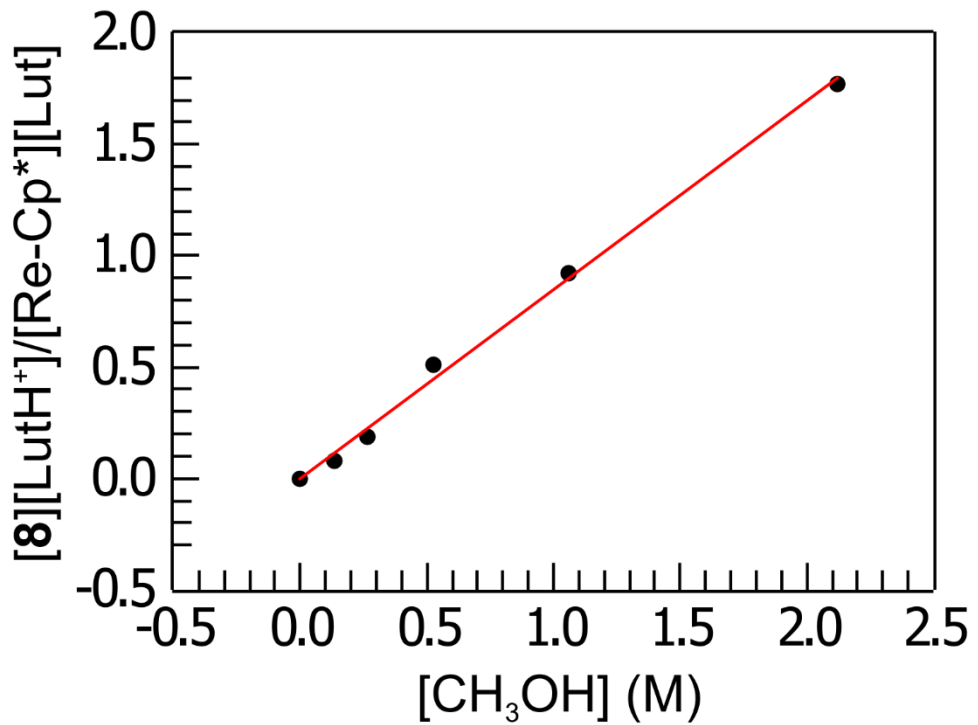


Figure S4. Plot of the ratio $[8][\text{LutH}^+]/[\text{Re-Cp}^*][\text{Lut}]$ (LutH^+ = 2,6-lutidinium, Lut = 2,6-lutidine, $\text{Re-Cp}^* = [\text{Re}(\eta^5-\text{Cp}^*)(\text{CO})_2(\text{NO})]^+$) present at equilibrium when $[\text{Re}(\eta^5-\text{Cp}^*)(\text{CO})_2(\text{NO})](\text{BF}_4^-)$ (6.5 mM) is treated with varying concentrations of CH₃OH in the presence of 2,6-lutidine (ca. 6.5 mM) in CD₃CN. The slope of the best-fit line gives K_{eq} .

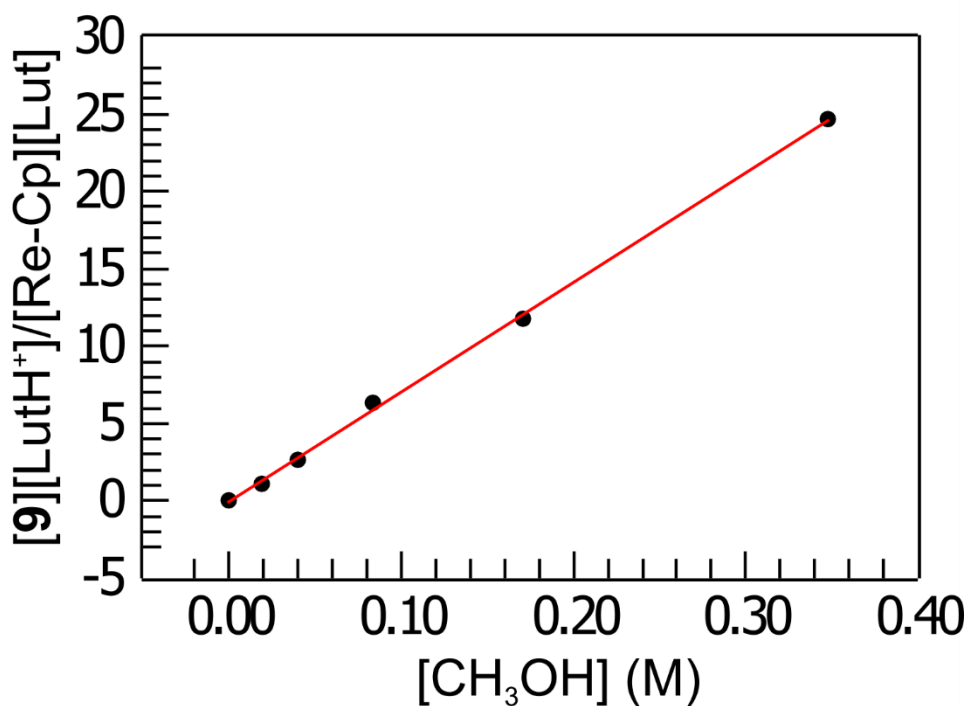


Figure S5. Plot of the ratio $[9][\text{LutH}^+]/[\text{Re-Cp}][\text{Lut}]$ (LutH^+ = 2,6-lutidinium, Lut = 2,6-lutidine, Re-Cp = $[\text{Re}(\eta^5\text{-Cp})(\text{CO})_2(\text{NO})]^+$) present at equilibrium when $[\text{Re}(\eta^5\text{-Cp})(\text{CO})_2(\text{NO})](\text{BF}_4^-)$ (5.9 mM) is treated with varying concentrations of CH₃OH in the presence of 2,6-lutidine (ca. 5.5 mM) in CD₃CN. The slope of the best-fit line gives K_{eq} .

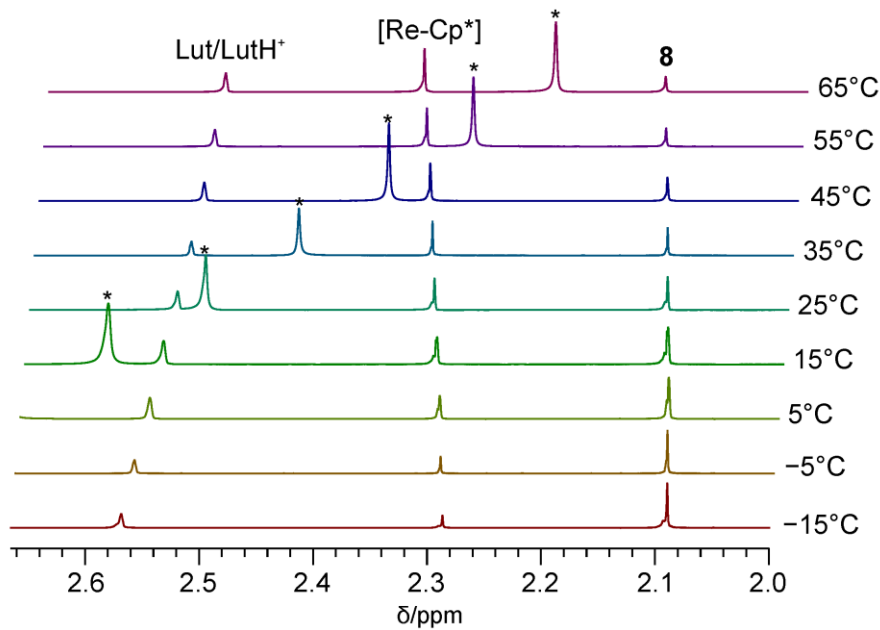


Figure S6. Partial variable-temperature ^1H NMR spectra for complex $[\text{Re}(\eta^5-\text{Cp}^*)(\text{CO})_2(\text{NO})](\text{BF}_4)$ (abbreviated $[\text{Re}-\text{Cp}^*]$) in the presence of 1 equivalent of 2,6-lutidine with 0.79 M CH_3OH in CD_3CN . The upfield region is shown, with peaks attributed to **8**, $[\text{Re}-\text{Cp}^*]$, and the averaged peak for 2,6-lutidine/2,6-lutidinium (Lut/LutH^+) labeled. Peaks for the OH group of the added methanol are labeled with an asterisk (*).

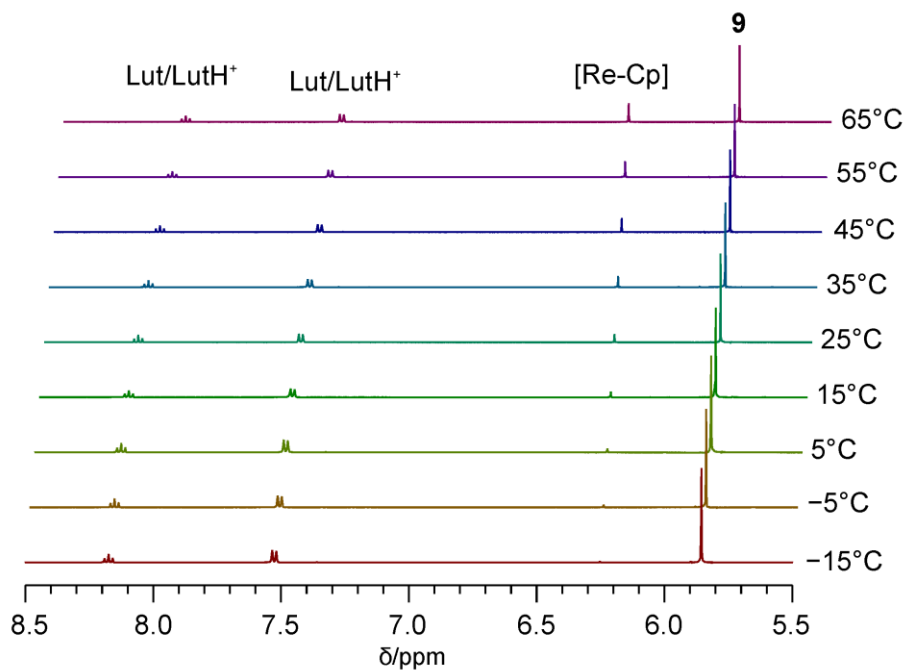


Figure S7. Partial variable-temperature ¹H NMR spectra for complex $[\text{Re}(\eta^5\text{-Cp})(\text{CO})_2(\text{NO})](\text{BF}_4)$ (abbreviated $[\text{Re}-\text{Cp}]$) in the presence of 1 equivalent of 2,6-lutidine with 0.79 M CH_3OH in CD_3CN . The downfield region is shown, with peaks attributed to **9**, $[\text{Re}-\text{Cp}]$, and the averaged peaks for 2,6-lutidine/2,6-lutidinium (Lut/LutH^+) labeled.

